Freeze drying WO_3 nanostructures for photocatalyst degradation of Rhodamine B dye from aqueous solution

Nguyen Thi Hoai Phuong[1*], Nguyen Duy Hung[2], Nguyen Cong Tu[2], Ngo Minh Tien[3], Tran Van Khanh[3]

[1]Joint Vietnam-Russia Tropical Science and Technology Research Center, 63 Nguyen Van Huyen, Nghia Do, Hanoi, Vietnam;
[2]Faculty of Engineering Physics, Hanoi University of Science and Technology, 1 Dai Co Viet, Bach Mai, Hanoi, Vietnam;
[3]Institute of Materials, Biology and Environment, Academy of Military Science and Technology, 17 Hoang Sam, Nghia Do, Hanoi, Vietnam.
[*]Corresponding author: hoaiphuong1978@gmail.com
Received 29 Jul. 2025; Revised 30 Sep. 2025; Accepted 16 Oct. 2025; Published 18 Nov. 2025.
DOI: https://doi.org/10.54939/1859-1043.j.mst.IMBE.2025.95-101

ABSTRACT

This study reports the synthesis and evaluation of tungsten oxide (WO_3) nanostructures prepared by a controlled hydrothermal method combined with freeze-drying for efficient Rhodamine B (RhB) degradation. The materials were characterized using XRD, SEM, and UV-Vis DRS, confirming a hexagonal crystal structure and strong visible-light absorption. Photocatalytic performance was examined under simulated sunlight, showing rapid RhB degradation with over 90% removal achieved within 120 minutes. Kinetic analysis indicated pseudo-first-order behavior, consistent with typical photocatalytic processes. The catalyst also exhibited excellent reusability and stability, maintaining more than 90% efficiency after three cycles and over 80% after seven cycles. These results demonstrate that freeze-drying effectively preserves porous nanostructures and enhances photocatalytic performance. Overall, the synthesized WO_3 nanostructures represent a cost-effective, durable, and sustainable photocatalyst with significant potential for wastewater treatment, contributing to the advancement of visible-light-driven advanced oxidation processes for environmental remediation.

Keywords: Tungsten trioxide (WO_3); Photocatalysis; Rhodamine B degradation; Hydrothermal synthesis; Advanced oxidation process; Wastewater treatment.

1. INTRODUCTION

The rapid expansion of industrial activities, particularly in the textile, printing, and dyeing sectors, has led to the widespread release of synthetic dyes into water bodies, posing a serious threat to aquatic ecosystems and human health [1]. Among various dyes, Rhodamine B (RhB), a xanthene-based dye, is widely used due to its high stability and brilliant color properties [2]. However, RhB is also known for its toxicity, carcinogenicity, and resistance to biodegradation, making it a persistent pollutant in wastewater [3]. Traditional methods like coagulation, adsorption, and biological degradation often do not fully remove complex dye molecules [4], which increases the demand for better wastewater treatment technologies.

Photocatalysis, a subset of advanced oxidation processes (AOPs), has emerged as a highly efficient and environmentally friendly approach for degrading organic pollutants in water [5]. Photocatalysis uses semiconductors to generate reactive oxygen species under solar or artificial light, degrading pollutants. TiO_2 is widely studied, but its large bandgap limits activity to UV, which represents only a small fraction of solar radiation [6]. Therefore, visible-light-responsive materials such as tungsten trioxide (WO_3) have gained increasing attention [7, 8]. WO_3, with a 2.6–2.8 eV bandgap, strong visible absorption, and good stability, is promising for solar photocatalysis [9, 10]. WO_3 synthesized from sodium tungstate via the hydrothermal method with

HCl showed a small size, broad light absorption, and low recombination, achieving 87% RhB degradation in 180 min [11]. A titanium-assisted method creating oxygen vacancies in WO_3 enhanced RhB degradation to 100% under simulated sunlight, versus ~ 60% for unmodified WO_3 [12]. WO_3 efficiency is hindered by recombination and limited sites; optimizing synthesis, structure, morphology, and surface features is vital for improvement.

WO_3 nanomaterials can be synthesized using diverse techniques, including sol–gel [13], acid precipitation [14], chemical vapor deposition [15], and hydrothermal synthesis [16], each affecting the material's shape, crystallinity, and photocatalytic efficacy. WO_3 nanostructures with enhanced visible-light absorption and accessible active sites are produced using hydrothermal synthesis and freeze-drying, enhancing photocatalytic efficacy and stability for dye degradation. Stopping collapse and aggregation during solvent removal with freeze-drying retains nanomaterials' porous and high-surface-area design [17, 18]. This approach creates compact, evenly distributed structures that absorb more light and react better for photocatalytic applications. Freeze-dried nanostructures can also assist the catalyst in accessing active sites and work better with pollutant compounds.

In this study, WO_3 nanostructures were synthesized and processed through freeze-drying to enhance their photocatalytic performance in degrading Rhodamine B from aqueous solutions under simulated sunlight. The freeze-dried WO_3 was carefully studied for its structural, morphological, and optical properties. Photocatalytic studies were performed to determine how efficiently and quickly the material breaks down Rhodamine B. The material's reusability and stability suggested it could be a cost-effective and efficient wastewater photocatalyst.

2. EXPERIMENTS

2.1. Chemicals

Natri tungstat dihydrat ($Na_2WO_4 \cdot 2H_2O$, 99.5%), Rhodamine B ($C_{28}H_{31}ClN_2O_3$, 99.5%), hydrochloric acid (HCl, 37%), and nitric acid (HNO_3, 65%) were procured from Merck, Germany.

2.2. Preparation of material

WO_3 materials were prepared through a facile hydrothermal method [19]. First, 8.25 g of $Na_2WO_4 \cdot 2H_2O$ was distributed in 25 mL of distilled water, then 3.2 mL of HNO_3 was slowly added. The mixture was swirled at room temperature for 30 minutes to generate a yellow suspension. To make the solution 80 mL, 36.8 mL of pure water was added. After stirring for 1 hour, the suspension was hydrothermally treated at 120 °C for 24 hours in a Nabertherm muffle furnace (Model: L9/11/B410, Germany). The formation of WO_3 was explained via the following equations [10]:

$$Na_2WO_4 + 2HNO_3 \rightarrow H_2WO_4 + 2NaNO_3 \quad (1)$$

$$H_2WO_4 \text{ (hydrothermal treatment, 120°C/24 h)} \rightarrow WO_3(s) + H_2O \quad (2)$$

The obtained precipitate was washed several times with distilled water, freeze-dried at - 60 °C for 24 hours using a DN-10N Desktop Freeze Dryer (China), and then ground into powder.

2.3. Characterization of material

WO_3 nanostructure was characterized using X-ray diffraction (XRD) with CuKα radiation (1.54 Å) over a 2θ range of 10°–70° (X'Pert Pro Panalytical). Surface morphology was observed via scanning electron microscopy (Hitachi S-4600). Raman spectroscopy (Renishaw Invia, 633 nm laser, 6.25 mW, 30 s) analyzed crystal features from 100–1200 cm^{-1}. Optical properties were assessed using diffuse reflectance spectroscopy (JASCO V-750) with a 60 mm integrating sphere at 200 nm/min scan speed and 5.0 nm bandwidth.

2.4. Rhodamine B photodegradation

The effectiveness of WO_3 as a catalyst was tested in a laboratory experiment aimed at breaking down RhB (Rhodamine B). In this standard experiment, 20 mL of a 5 mg/L RhB solution was

prepared. A catalyst concentration of 0.5 g/L of WO_3 was added to the solution. Before light irradiation, the suspension containing WO_3 and RhB was kept in the dark for 30 minutes to establish adsorption–desorption equilibrium. A 350 W xenon lamp was used to simulate sunlight, with the samples placed 15 cm from the lamp to ensure consistent irradiation. The solution temperature was maintained at (25 ± 2)°C using an air cooling system, with the RhB solution at its autogenous initial pH. Samples were filtered to remove the solid catalyst at 0, 30, 60, 90, and 120 minutes. The solution's residual RhB concentration was measured with a UV-Vis spectrophotometer at 552 nm. RhB elimination efficiency on WO_3 was computed using this equation [20]:

$$H\% = \frac{(C_0 - C_t)}{C_0} \times 100\% \quad (3)$$

where C_0 and C_t were determined from UV-Vis absorbance at 552 nm using a RhB calibration curve with the regression equation C = 5.56938×Abs – 0.09263.

After each cycle, WO_3 was filtered, washed with distilled water to remove residual dye, dried at 60 °C, and reused.

3. RESULTS AND DISCUSSION

3.1. Characterization of freeze-dried WO_3 nanostructure

Figure 1 SEM pictures reveal the porous, flower-like morphology of freeze-dried WO_3 nanostructures, with interconnecting nanosheets and nanorods clustered together. These nanorod bundles form three-dimensional architectures with wrinkled and crumpled textures, creating a highly open structure with a vast surface area. Nanorod clustering improves structural stability, light harvesting, and reactant diffusion. The material is ideal for surface-related applications like photocatalysts because its structure remains intact after freeze-drying, minimizing clumping and increasing active site availability.

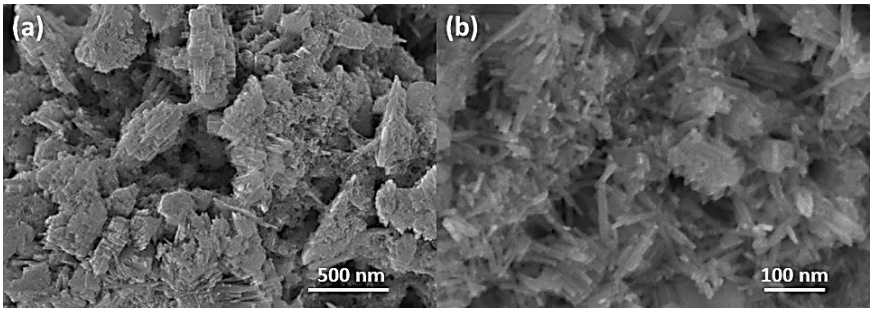

Figure 1. *SEM images of freeze-drying WO_3 nanostructures.*

XRD pattern and UV-Vis spectrum were used to analyze freeze-dried sample physicochemical properties (figures 2a and 2b). Free-dried sample XRD pattern matches hexagonal WO_3 structure (ICDD card no 01-075-2187). The peaks at 2θ of ~14.0, 22.8, 24.4, 26.8, 28.2, 33.6, and 36.6° correspond to x-ray diffraction from (100), (001), (110), (101), (200), (111), and (201) planes in hexagonal WO_3. Free-dried sample XRD showed no additional phases or impurities. Free-dried sample's diffuse reflectance spectrum (figure 2b) with visible-light edge suggests it absorbs visible light.

Further analysis of the reflectance spectra of the sample using Kubelka-Munk equation (Eq. 4) [21, 22]:

$$[F(R) \times hv]^n = A(hv - E_g) \quad (4)$$

where F(R) = (1−R)2/2R, where R is diffuse reflectance, hv is input photon energy, A is an arbitrary coefficient, Eg is the sample optical bandgap, and n = 2 and ½ for direct and indirect permitted recombination. For WO_3, an indirect-bandgap semiconductor, n = ½ [22, 23]. The optical

bandgap of the sample was extrapolated from the Kubelka-Munk plots $[F(R)\times hv]^{1/2}$ vs. hv (the inset in figure 2b), which is 2.70 eV in the visible range. The visible-range optical bandgap makes the free-dried sample suitable for solar-driven applications.

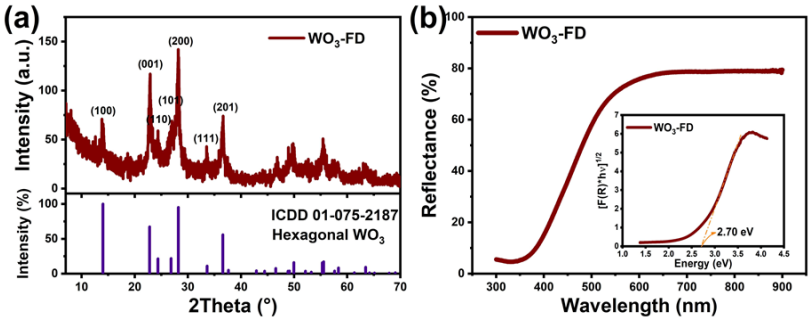

Figure 2. *XRD pattern (a) and UV-Vis DRS spectroscopy (b) of freeze-drying WO_3 nanostructures. The inset is the Kubelka-Munk plot.*

Figure 3 shows the EDX spectrum and elemental composition of freeze-dried WO_3 nanostructures. The effective synthesis of WO_3 is proven by substantial tungsten (W) and oxygen (O) peaks, with minimal sodium (Na) present. Analysis shows high tungsten (73.49 weight percent, 19.77 atomic percent) and oxygen (24.67 weight percent, 76.27 atomic percent) content, indicating WO_3 composition. WO_3 photocatalytic activity is unaffected by low Na levels, and alkali metal ions may alter crystal formation, according to research. The high oxygen atomic fraction suggests fully oxidized tungsten. Freeze-drying preserved the purity and integrity of WO_3 nanostructures, as seen by the equal distribution of elements in SEM-EDX mapping.

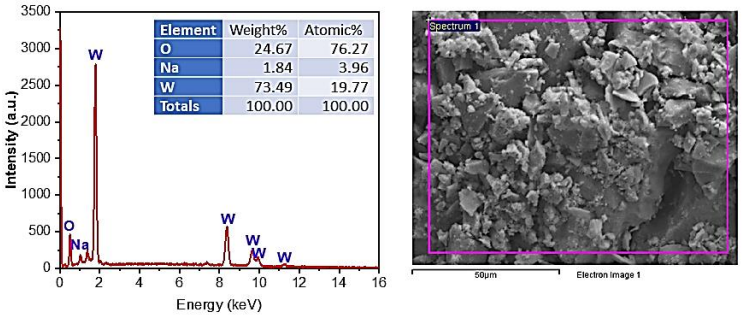

Figure 3. *EDX spectroscopy of freeze-drying WO_3 nanostructures.*

3.2. Photodegradation of Rhodamine B on freeze-dried WO_3 nanostructure

Figure 4 shows Rhodamine B (RhB) breakdown by freeze-dried WO_3 nanostructures in simulated sunlight.

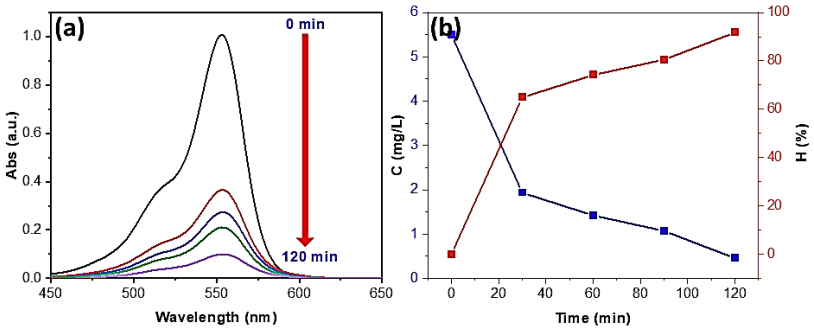

Figure 4. *UV-Vis spectroscopy (a) and concentration, photodegradation efficiency (b) of Rhodamine B vs time on freeze-drying WO_3 nanostructures.*

In figure 4a, the UV-Vis absorption spectra show that RhB's 552 nm absorption peak is decreasing over time, indicating dye degradation. In 120 minutes, RhB content dropped from 5.50 mg/L to 0.46 mg/L, increasing degradation efficiency (H) from 0% to 91.7% (figure 4b). The quick decrease in absorbance and concentration, especially in the first 30 min, indicates the photocatalytic activity of WO_3 nanostructures. The virtually linear increase in H (%) after 30 min indicates continuing reactive species formation, highlighting WO_3's potential as an effective photocatalyst for dye-contaminated wastewater treatment.

Figure 5 illustrates the kinetic modeling of Rhodamine B (RhB) photodegradation using freeze-dried WO_3 nanostructures [24]. The pseudo-first-order model (figure 5a) shows a linear plot of $\ln(C_0/C_t)$ versus time with a good correlation value ($R^2 = 0.94406$). The slope of 0.01855 min^{-1} supports a computed rate constant k_1 of 0.0427 min^{-1}, aligning well with experimental results. On the other hand, the pseudo-second-order model (figure 5b) has a lower correlation value ($R^2 = 0.83038$) and a slope of 0.01476 $L \cdot mg^{-1} \cdot min^{-1}$, resulting in $k_2 = 0.00134$ $L \cdot mg^{-1} \cdot min^{-1}$. The first-order model better explains RhB degradation on WO_3 nanostructures, indicating that dye concentration, not active site number, is the primary factor. According to M. B. Tahir et al. (2018) and Y. Zhang et al. (2023), the photocatalytic mechanism of RhB degradation by WO_3 under visible light involves photon absorption, electron-hole pair generation, and the production of free radicals (•OH, $•O_2^-$) [11, 12]. Results indicate pseudo-first-order kinetics in degradation, demonstrating the effectiveness of the produced WO_3 photocatalyst in simulated sunlight.

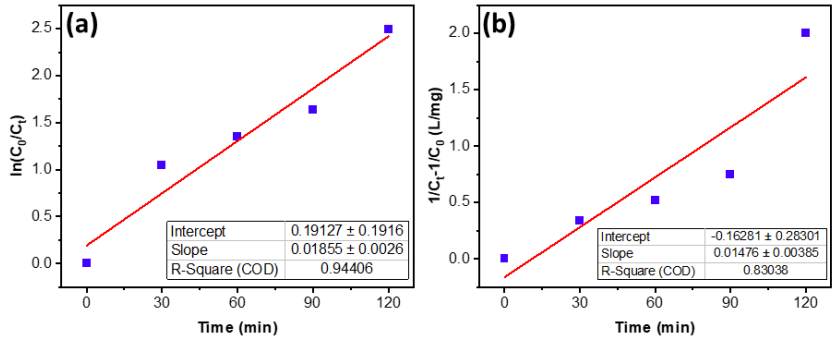

Figure 5. *The first-pseudo order (a) and second-pseudo order (b) of photodegradation of Rhodamine B on freeze-drying WO_3 nanostructures.*

3.3. Reusability of freeze-dried WO_3 nanostructure

Reuse of freeze-dried WO_3 nanostructures for Rhodamine B degradation across seven cycles is demonstrated in figure 6.

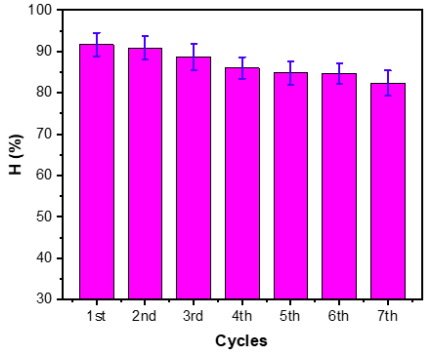

Figure 6. *Reusability of freeze-dried WO_3 nanostructure for photodegradation of Rhodamine B.*

H started at 91.69% in the first cycle and dropped to 82.34% on the seventh. The WO_3 photocatalyst remains stable for photocatalytic processes, maintaining ~ 90% efficiency after three

uses and over 80% efficiency after seven uses, despite a slight performance decline. Small error range fluctuations (2.5–3.2%) indicate reproducible performance. Partial surface fouling, active site blockage, or modest structural changes following frequent use cause the progressive deterioration. Under simulated sunlight, the material showed good durability and reusability, suggesting it could be used in dye-contaminated wastewater treatment.

4. CONCLUSIONS

This study found that WO_3 nanostructures may be manufactured using hydrothermal and freeze-drying methods. Flower-shaped materials with porous nanorod bundles were developed. WO_3 analysis revealed a hexagonal structure, high visible light absorption, and a 2.70 eV bandgap, making it ideal for photocatalytic applications. Under 120 minutes, freeze-dried WO_3 effectively degraded Rhodamine B, eliminating almost 91% of it under simulated sunlight. Kinetic investigation showed a pseudo-first-order kinetics model with a strong correlation coefficient for deterioration. The photocatalyst was stable and reusable, maintaining 90% efficiency after seven cycles. These findings indicate that freeze-dried WO_3 nanostructures are a cost-effective and eco-friendly photocatalyst for wastewater treatment. To enhance the effectiveness of WO_3 in treating difficult organic contaminants, future research should focus on improving its ability to absorb light and separate charges through new structures or surface changes.

Acknowledgment: *This research was financed by the National Foundation for Science and Technology Development under grant code NCUD.01-2024.15 and conducted at the Joint Vietnam-Russia Tropical Science and Technology Research Center.*

REFERENCES

[1]. Sharma, J., Sharma, S., and Soni, V. *"Classification and impact of synthetic textile dyes on aquatic flora: A review."* Regional Studies in Marine Science, vol. 45, p. 101802, (2021).

[2]. Guan, Y., Wu, W., Su, J., and Zhang, L. *"Synthesis of rhodamine B amine derivatives with improved light resistance and its application in thermochromic materials."* Dyes and Pigments, vol. 233, p. 112529, (2025).

[3]. Ismail, M., et al. *"Pollution, toxicity and carcinogenicity of organic dyes and their catalytic bio-remediation."* Current Pharmaceutical Design, vol. 25, no. 34, pp. 3645–3663, (2019).

[4]. Al-Tohamy, R., et al. *"A critical review on the treatment of dye-containing wastewater: Ecotoxicological and health concerns of textile dyes and possible remediation approaches for environmental safety."* Ecotoxicology and Environmental Safety, vol. 231, p. 113160, (2022).

[5]. Iqbal, M. A., et al. *"Advanced photocatalysis as a viable and sustainable wastewater treatment process: A comprehensive review."* Environmental Research, vol. 253, p. 118947, (2024).

[6]. Suhaimi, N. H. S., et al. *"Recent updates on TiO_2-based materials for various photocatalytic applications in environmental remediation and energy production."* Desalination and Water Treatment, vol. 321, p. 100976, (2025).

[7]. Huang, J., Yue, P., Wang, L., She, H., and Wang, Q. *"A review on tungsten-trioxide-based photoanodes for water oxidation."* Chinese Journal of Catalysis, vol. 40, no. 10, pp. 1408–1420, (2019).

[8]. Raub, A. A. M., Bahru, R., Nashruddin, S. N. A. M., and Yunas, J. *"Advances of nanostructured metal oxide as photoanode in PEC water splitting application."* Heliyon, vol. 10, no. 20, (2024).

[9]. Nguyen, H. S., et al. *"Ag-decorated novel h'-WO_3 nanostructures for sustainable applications."* Journal of Materials Science, vol. 48, no. 13, pp. 18687–18698, (2022).

[10]. Pham, N. L. et al., *"Temperature-mediated phase transformation and optical properties of tungsten oxide nanostructures prepared by hydrothermal method."* Materials Chemistry and Physics, vol. 32, no. 3, pp. 307–307, (2022).

[11]. Tahir, M. B., et al. *"WO_3 nanostructures-based photocatalyst approach towards degradation of RhB dye."* Journal of Materials Science: Materials in Electronics, vol. 28, no. 3, pp. 1107–1113, (2018).

[12]. Zhang, Y., et al. *"Novel synthesis method of oxygen vacancy WO_3 and its photocatalytic performance for degradation of rhodamine B."* Ceramics International, vol. 98, no. 6, pp. 1542–1550, (2023).

[13]. Zhang, G., et al. *"Effects of annealing temperature on optical band gap of sol–gel tungsten trioxide films."* Journal of Sol-Gel Science and Technology, vol. 9, no. 8, p. 377, (2018).
[14]. Gorobtsov, P. Y., et al. *"Synthesis of nanoscale WO_3 by chemical precipitation using oxalic acid."* Russian Journal of Inorganic Chemistry, vol. 66, no. 12, pp. 1811–1816, (2021).
[15]. Nakrela, A., et al. *"Comprehensive investigation of WO_3-x thin films: Structural, optical, and electrical insights, with application in photodegradation of dyes."* Journal of Materials Research and Technology, (2025).
[16]. Jamali, M., Tehrani, F. S., and B. E. *"Thermally stable WO_3 nanostructure synthesized by hydrothermal method without using surfactant."* Materials Science, vol. 270, p. 115221, (2021).
[17]. Ma, Y., et al. *"Synthesis of superhydrophobic crack-free monolithic silica aerogels via a vacuum freeze-drying process."* Journal of the American Ceramic Society, vol. 108, no. 6, p. e20401, (2025).
[18]. Trenkenschuh, E. *"Freeze-drying of nanoparticles: Impact of particle properties on formulation and process development."* LMU Dissertation, (2021).
[19]. L. T. L., et al. *"Synthesized and characterization of WO_3 nanorod hybridization Gr application in environmental treatment."* Results in Engineering, vol. 90, (2021).
[20]. Zhu, Q., et al. *"Efficient photocatalytic removal of RhB, MO and MB dyes by optimized Ni/NiO/TiO_2 composite thin films under solar light irradiation."* Materials Today: Proceedings, vol. 6, no. 2, pp. 2724–2732, (2018).
[21]. Nguyen, K. D., et al. *"Facile one-step synthesis of in situ WO_3@Gr nanorods as an efficient material for antimicrobial and decoloration applications."* Nanotechnology, vol. 15, no. 2, p. 025009, (2024).
[22]. Pham, N. L., Luu, T. L. A., Nguyen, H. L., Nguyen, C. T. *"Effects of acidity on the formation and adsorption activity of tungsten oxide nanostructures prepared via the acid precipitation method."* Materials Chemistry and Physics, vol. 272, p. 125014, (2021).
[23]. Duan, G., et al. *"Robust antibacterial activity of tungsten oxide (WO_3-x) nanodots."* Colloids and Surfaces B: Biointerfaces, vol. 32, no. 7, pp. 1357–1366, (2019).
[24]. Luu, T. L. A., et al. *"Graphene oxide-wrapped tungsten trioxide for adsorptive removal of methylene blue."* Materials Chemistry and Physics, vol. 316, p. 129033, (2024).

TÓM TẮT

Nghiên cứu chế tạo xúc tác quang WO_3 xử lý thuốc nhuộm Rhodamine B trong nước

Nghiên cứu này báo cáo quá trình tổng hợp và đánh giá các cấu trúc nano oxit vonfram (WO_3) được chế tạo bằng phương pháp thủy nhiệt có kiểm soát kết hợp với sấy thăng hoa để phân hủy Rhodamine B (RhB) hiệu quả. Các vật liệu được đặc trưng bằng XRD, SEM và UV-Vis DRS, xác nhận cấu trúc tinh thể lục giác và khả năng hấp thụ ánh sáng khả kiến mạnh. Hiệu suất quang xúc tác được kiểm tra dưới ánh sáng mặt trời mô phỏng, cho thấy sự phân hủy RhB nhanh chóng với hơn 90% loại bỏ đạt được trong vòng 120 phút. Phân tích động học cho thấy hành vi giả bậc nhất, phù hợp với các quá trình quang xúc tác thông thường. Chất xúc tác cũng thể hiện khả năng tái sử dụng và độ ổn định tuyệt vời, duy trì hiệu suất hơn 90% sau ba chu kỳ và hơn 80% sau bảy chu kỳ. Những kết quả này chứng minh rằng sấy thăng hoa bảo quản hiệu quả các cấu trúc nano xốp và tăng cường hiệu suất quang xúc tác. Nhìn chung, các cấu trúc nano WO_3 tổng hợp đại diện cho chất xúc tác quang bền vững, tiết kiệm chi phí và có tiềm năng đáng kể trong xử lý nước thải, góp phần thúc đẩy các quy trình oxy hóa nâng cao sử dụng ánh sáng khả kiến để phục hồi môi trường.

Từ khoá: Vonfram trioxide (WO_3); Quang xúc tác; Phân hủy Rhodamine B; Kỹ thuật thủy nhiệt; Quy trình oxy hóa nâng cao; Xử lý nước thải.